

RSC Advances



This is an *Accepted Manuscript*, which has been through the Royal Society of Chemistry peer review process and has been accepted for publication.

Accepted Manuscripts are published online shortly after acceptance, before technical editing, formatting and proof reading. Using this free service, authors can make their results available to the community, in citable form, before we publish the edited article. This *Accepted Manuscript* will be replaced by the edited, formatted and paginated article as soon as this is available.

You can find more information about *Accepted Manuscripts* in the [Information for Authors](#).

Please note that technical editing may introduce minor changes to the text and/or graphics, which may alter content. The journal's standard [Terms & Conditions](#) and the [Ethical guidelines](#) still apply. In no event shall the Royal Society of Chemistry be held responsible for any errors or omissions in this *Accepted Manuscript* or any consequences arising from the use of any information it contains.

Enhancement of Interfacial Interaction between Poly(vinyl chloride) and Zinc Oxide Modified Reduced Graphene Oxide

Ping Li¹ Xudong Chen^{1,2} Jian-Bing Zeng¹ Lin Gan¹ Ming Wang^{1*}

¹School of Chemistry and Chemical Engineering, Southwest University, Chongqing, 400715, China

²Key Laboratory of Polymer Composite and Function Materials of Ministry of Education, Key Laboratory for Designed Synthesis and Applied Polymer Materials, School of Chemistry and Chemical Engineering, Sun Yat-sen University, Guangzhou, 510275 China.

Abstract

To obtain the satisfied performance of the polymer/graphene composite, it is extremely important to improve the interfacial interaction between the filler and the polymeric matrix. In this study, we aimed to enhance the interfacial interaction between poly (vinyl chloride) (PVC) and reduced graphene oxide (rGO) by decorating rGO with zinc oxide (ZnO) nanoparticles. A one-pot chemical route for the synthesis of rGO loaded with ZnO nanoparticles (rGO-ZnO) was achieved by mixing graphene oxide (GO) and Zinc nitrate ($\text{Zn}(\text{NO}_3)_2$) in water and then gradually adding sodium hydroxide and hydrazine hydrate. The resulting rGO-ZnO hybrid was characterized by scanning electron microscopy (SEM), transmission electron microscopy (TEM), electrochemical analysis and X-ray diffraction (XRD). The PVC/rGO-ZnO composites were fabricated by a simple solution mixing and drop casting. The enhancement of interfacial

*Corresponding Author. Tel/Fax: 0086-023-68254000.
E-mail address: mwang@swu.edu.cn (M. Wang)

interaction between PVC and rGO-ZnO was evaluated by tensile test, interfacial tension and glass transition analysis. The results revealed that the ZnO nanoparticles acted as a 'bridge', connecting with PVC via electrostatic attraction/hydrogen bonding and connecting with rGO by p - π stacking/electrostatic interaction. Thanks to the strong interfacial interaction, both the mechanical properties and the glass transition temperature were significantly enhanced.

Keywords Poly(vinyl chloride), Reduced graphene oxide, Zinc oxide, Interfacial strength, Mechanical properties

1. Introduction

Poly(vinyl chloride) (PVC) has been widely used as a host polymer matrix for preparing polymeric composite materials during the past decades because of its low cost and excellent chemical stability and biocompatibility [1]. The present challenge for producing high performance polymeric composites lies in the selection of the desirable reinforcing filler, which can be well dispersed in the polymer matrix while rendering strong interfacial interaction with the matrix. So far, clay [2], cellulose whiskers [3], calcium carbonate [4], and carbon nanotubes [5] are often used as fillers to prepare functional polymeric composites with high mechanical strength.

Graphene, a rising star in the carbon family, has become one of the most exciting materials nowadays due to its unique mechanical, electronic and optical properties [6-8]. Considerable efforts have been directed towards the development of graphene-reinforced functional polymeric composites [9, 10]. It has been demonstrated in previous reports that the maximum improvements in final properties can be achieved

when graphene is homogeneously dispersed in the matrix and the external load is efficiently transferred through strong graphene/polymer interfacial interactions [11, 12]. However, the hydrophobic nature of pristine graphene engenders weak interfacial interactions with the hydrophilic polymer matrix (such as PVC) as well as its poor dispersion in the matrix, limiting the performance of the composites. Therefore, to achieve the satisfied performance of the graphene/polymer composite, it is extremely important to improve their compatibility and the interfacial interaction between the filler and the polymeric matrix.

In previous studies, it was demonstrated that the incorporation of metal oxide such as ZnO particles in PVC led to the mechanical improvement [13, 14], because the ZnO particles have strong interaction with the PVC chains. Furthermore, PVC blended with ZnO can suppress the emission of toxic chemicals such as carcinogenic dioxins and hydrochloric acid by the photocatalytic degradation compared to the degradation of waste plastics in conventional incinerators [14]. On the other hand, metal oxides such as Fe_3O_4 [15, 16] and CuO [17, 18] have also been anchored onto graphene oxide (GO) or reduced GO (rGO) sheets to form novel hybrid materials, demonstrating a range of unique and useful properties.

In this work, we demonstrate the preparation of a kind of graphene-reinforced PVC composite by introducing the ZnO particles to bridge graphene sheets and the PVC matrix. The incorporation of ZnO not only renders the good dispersion of graphene sheets in the PVC matrix, but also improves the interfacial interaction between graphene and PVC. The resultant PVC/rGO-ZnO composites show enhanced mechanical

properties and increased glass transition temperature.

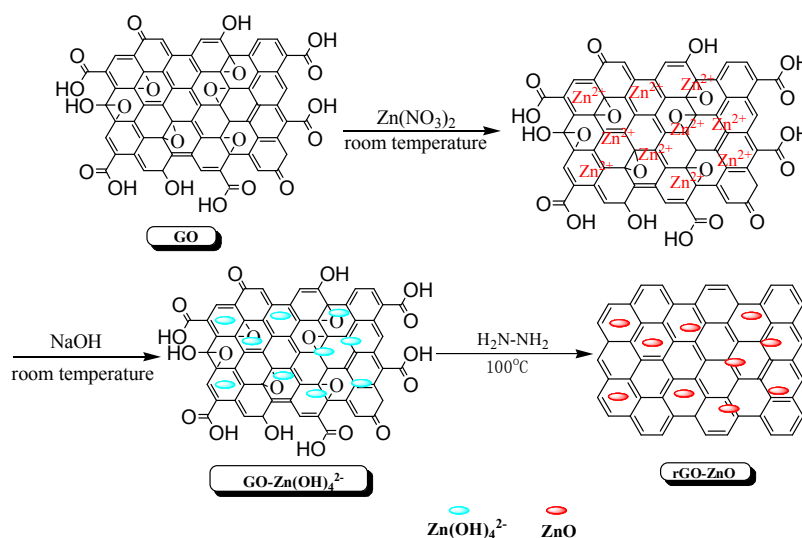
2. Experimental

2.1 Materials

The nature flake graphite was purchased from Nanyang Boxin Mining Ltd. Zinc nitrate hexahydrate ($\text{Zn}(\text{NO}_3)_2 \cdot 6\text{H}_2\text{O}$, 99.0 %) and sodium hydroxide (NaOH, 96.0 %) were obtained from Chengdu Kelong Chemical Reagent Factory. Hydrazine hydrate (80.0 % aq.), anhydrous ethanol ($\text{C}_2\text{H}_5\text{OH}$, 99.7 %) and tetrahydrofuran (THF, AR) were purchased from Chongqing Chuandong Chemical Co. Ltd. PVC was obtained from Sichuan Jinlu Resin Co. Ltd. Zinc oxide (ZnO , 99.0 %) was purchased from Tianjin Regent Chemicals Co. Ltd. Graphene nanoplatelets (GNPs, layers <30, size: 5-10 μm , thickness: 4-20 nm) were obtained from Chengdu Organic Chemicals Co. Ltd., Chinese Academy of Sciences.

2.2 Preparation of the rGO-ZnO hybrid materials

Typically, the GO (4 mL, 1.0 mg/mL in water), prepared by the Hummers method [19], and $\text{Zn}(\text{NO}_3)_2$ (4 mL, 0.3 M in water) were firstly mixed with ultrasonication to achieve a homogenous solution. Afterwards, a dilute NaOH solution was dropped into the above mixture solution at room temperature to form $\text{Zn}(\text{OH})_4^{2-}$ particles on GO surface. The hydrazine hydrate (2 mL) was added subsequently and the reaction mixture was kept at 100 °C for 24 h and finally formed a grayish-black suspension. The final product was centrifuged followed by washing with deionized water and ethanol for several times until pH=7, and drying in a vacuum oven at 60 °C. The fabrication process was illustrated in Scheme 1.



Scheme 1 Schematic of the preparation for the rGO-ZnO hybrid materials

2.3 Preparation of the PVC/rGO-ZnO nanocomposites

The PVC/rGO-ZnO nanocomposites were prepared by a solution-mixing method. In a typical experiment, the rGO-ZnO fillers were firstly dispersed in THF with ultrasonication and PVC was dissolved in THF to form a transparent and homogenous solution. After that, the above two kinds of solution were mixed under ultrasonication. Finally, the mixed solution was cast onto the glass plates and dried at 50 °C, forming a film with thickness of ca. 65 μm . To investigate the rGO-ZnO loading effect, the composites with 5, 10, 15 and 20 wt% rGO-ZnO hybrids were prepared, respectively. For comparison, PVC, ZnO and GNPs were directly mixed in THF and the mixture solution was cast to form the PVC/GNPs/ZnO composites with the same content. The molar amount of ZnO per unit mass of GNPs was kept the same with the molar amount of $\text{Zn}(\text{NO}_3)_2$ per unit mass of GO.

2.4 Characterization

The morphology of the rGO-ZnO hybrid was investigated by scanning electron

microscopy (SEM, S4800 Hitachi) at an accelerating voltage of 10 kV, and transmission electron microscopy (TEM, Tecnai G2 F20) at an accelerating voltage of 200 kV. For SEM observation, the sample was coated with a thin layer of gold before observation. For TEM observation, the sample was dispersed in ethanol with ultrasonication and then dripped onto copper grids. The crystal structure of rGO decorated with ZnO was characterized by an X-ray diffraction (Shimadzu XRD-7000), using a Cu K α radiation with a wavelength of 1.54 Å. The testing was performed over the angle range $2\theta=5-70^\circ$ with a scanning rate of 4 $^\circ$ /min. The photoluminescence spectra of the sample were studied on an F7000 fluorescence spectrophotometer with an excitation wavelength of 325 nm. The solid samples were compressed before testing. The cyclic voltammetry (CV) and electrochemical impedance spectroscopy (EIS) of the samples were studied by a CHI660D electrochemical workstation. A 3- electrode system was used to study the capacitive behavior with 2 M KOH as the electrolyte solution. Glassy carbon electrode (GCE, diameter $\Phi=4$ mm) was used as a working electrode. A platinum foil and Ag/AgCl electrode were used as the counter and reference electrodes, respectively. The EIS measurements were performed over the frequency range, 0.1 Hz to 100 kHz, at the open circuit potential with an ac perturbation of 5 mV.

To evaluate the interaction between the filler and PVC, the surface tension and glass transition temperature of the composites were tested. The glass transition temperature of PVC with the filler was investigated by differential scanning calorimetry (NETZSCH DSC 200 F3 Maia) using nitrogen as a purge gas. The samples (about 5 mg) were heated from 30 $^\circ$ C to 150 $^\circ$ C at a heating rate of 10 $^\circ$ C/min and maintained at 150

°C for 5 min to erase the thermal history, and cooled down to 30°C at the cooling rate of 10 °C/min. For the interfacial tension test, the contact angles of water and CH₂I₂ were measured with a contact angle tester (JC2000C1) at 23±2 °C. The mechanical properties of the PVC composite films were studied with an instron universal tensile testing machine with a cross-head speed of 10 mm/min. All the mechanical tests were carried out at room temperature (23±2 °C) and the average values from at least five samples were reported. The dispersion of rGO-ZnO in PVC matrix and the fracture behaviors of the samples were observed by SEM (S4800 Hitachi) at 10 kV. For the dispersion evaluation, the samples were firstly cryogenically fractured in liquid nitrogen, followed by the coating with a layer of gold. The samples were then observed by SEM equipped with Energy Dispersive Spectrometer (EDS). Both the morphology and the Zn element distribution of the samples were recorded. For the comparison of the fracture behavior, the tensile fractured surface was directly coated with a layer of gold prior to SEM observation.

3 Results and discussion

3.1 Characterization of rGO-ZnO

Figure 1 showed the XRD results of the ZnO, rGO-ZnO and GNPs/ZnO. The characteristic diffraction peaks of hexagonal ZnO (JCPDS card No. 36-1451) were observed in both diffraction patterns of rGO-ZnO and GNPs/ZnO, suggesting the successful formation of hexagonal ZnO during the hydrothermal process. The characteristic diffraction peak of GNPs at 26.6 ° was also found in the GNPs/ZnO particles under direct physical mixing. However, the characteristic peaks of rGO, which

were related to the disordered graphite nanocrystallites formed by the reduction reactions [20], were very weak and broad in rGO-ZnO. The results indicated that ZnO could not make GNPs be exfoliated under simply physical mixing, but could probably prevent the rGO sheets from restacking and agglomerating [21]. The results also illustrated that the rGO sheets were well exfoliated in the rGO-ZnO hybrids.

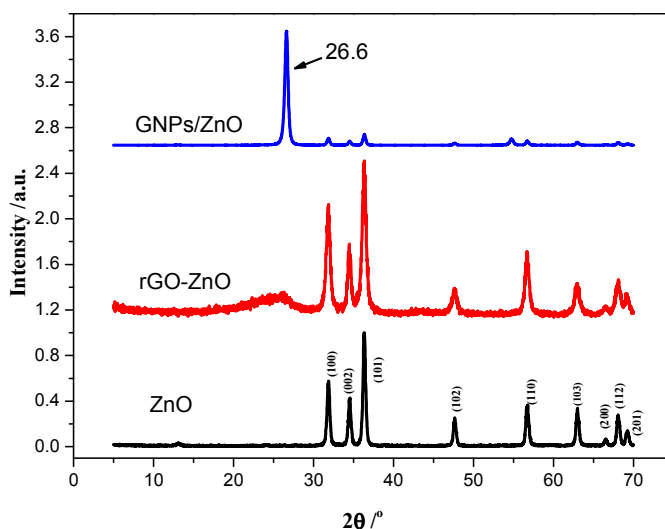
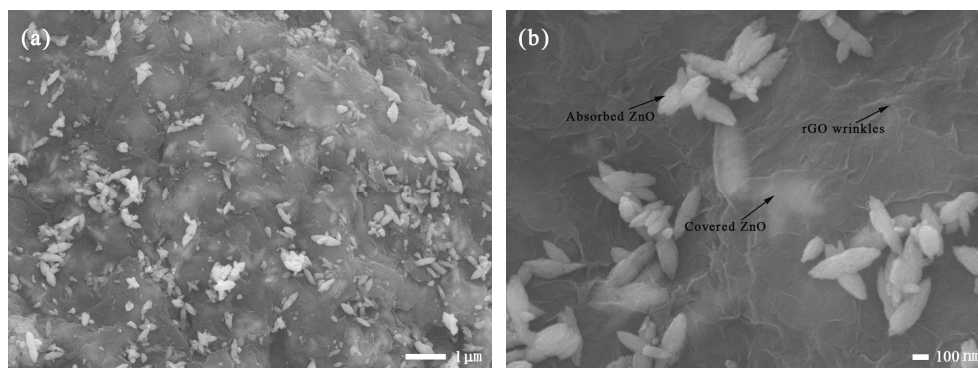


Figure 1 XRD patterns of ZnO, rGO-ZnO and GNPs/ZnO

Figure 2 shows the SEM and TEM images of rGO-ZnO hybrids and GNPs/ZnO particles. As can be seen, ZnO nanorods with an average width of 100 nm and an average length of 300 nm were uniformly distributed on the surface of rGO sheets (Figure 2b). The presence of the ZnO can prevent the rGO sheets from restacking and agglomerating. Moreover, the rGO sheets showed rough and wrinkling surface, which could probably improve the interaction with PVC chains. TEM observation also showed that the rGO surface was covered or embedded with the ZnO nanorods. The TEM images seemed to show more ZnO particles on the rGO surface than that of the SEM images. However, if we carefully observed the SEM images (Figure 2a and 2b) and

TEM images (Figure 2c), we could find the results were consistent. The reasons for the illusion were that the SEM images mainly gave the morphologies of the surface of the samples, while the TEM image gave the morphologies of the whole samples. Only a few of ZnO particles which are embedded in the rGO could be found in the SEM images. However, all the ZnO particles, no matter inside and outside of the rGO, could be seen in the TEM images. HRTEM image and the selected area electron diffraction (SAED) patterns (Figure 2d) revealed the intimate contact between ZnO nanorods and rGO.

The GNPs/ZnO particles which were prepared by directly mixing GNPs and ZnO particles were also investigated by SEM. The square-shaped ZnO crystals were aggregated on the surface of the GNPs. The surfaces of the GNPs were much smoother than that of the rGO surfaces, as shown in Figure 2e and 2f. The results indicated that the interfacial interaction between GNPs and ZnO was worse than that of rGO and ZnO in rGO-ZnO hybrids. Furthermore, the aggregation of ZnO and the smooth of GNPs were probably negative to enhance the mechanical and thermal properties of PVC.



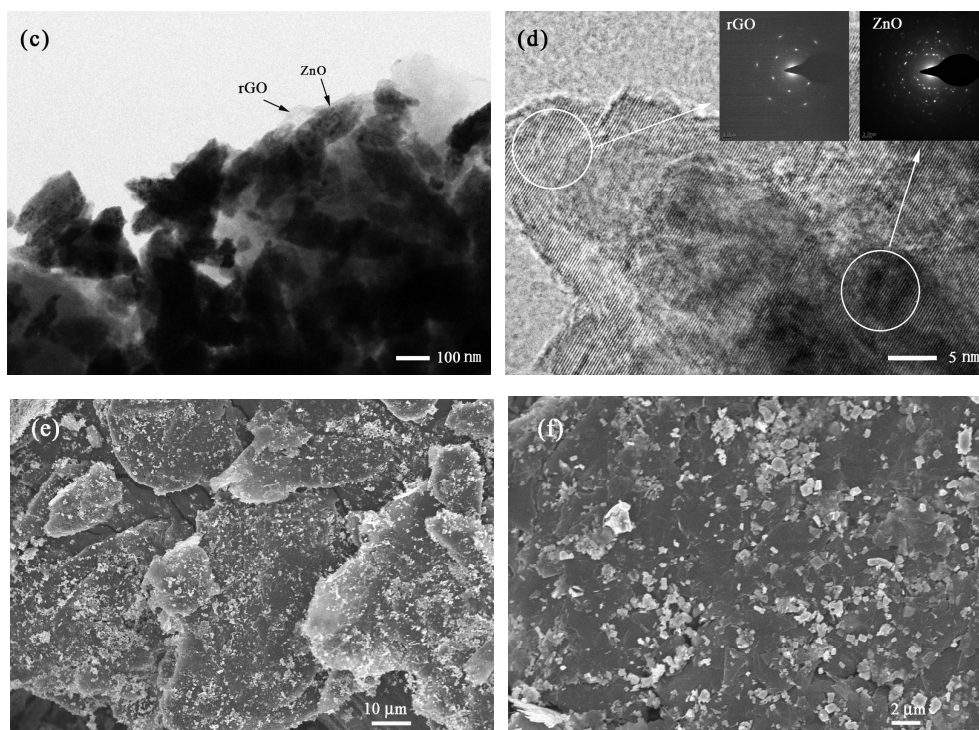


Figure 2 SEM images of the rGO-ZnO hybrid particles (a, b) and the GNPs/ZnO particles (e, f); TEM (c) and high resolution transmission microscopy (HRTEM) (d) images of the rGO-ZnO hybrid particles. Selected area electron diffraction (SAED) patterns are given in (d).

As is known, GO can exhibit fluorescence by destroying the π - π conjugated structure of graphene [22]. However, the reconstruction the π - π conjugated structure will quench the fluorescence of GO via chemical/physical reduction [23]. Figure 3 shows the fluorescent spectra of the ZnO, rGO-ZnO and GNPs/ZnO particles. As can be seen, the fluorescence spectrum of ZnO shows an emission peak at ~ 390 nm and a broadband emission peak at around 500 nm, similar to previous reports [24]. After the incorporation of GNPs by the physical blending, although the fluorescence intensity of the ZnO was significantly reduced, the two emission peaks at 390 and 550 nm still existed. In contrast, the ZnO fluorescence for the rGO-ZnO sample was almost completely quenched. Significantly, two emission peaks disappeared and a new emission peak appeared. It has been demonstrated that the recombination of

photogenerated carriers of ZnO can be effectively suppressed in the presence of carbon materials [25]. The interfacial connection between ZnO and carbon materials will reduce the probability of recombination and lead to an increased charge carrier separation. Thus, the complete quenching in rGO-ZnO should be ascribed to the enhancement of interfacial interaction between ZnO and carbon materials. This also implies that the interfacial interaction in the rGO-ZnO samples was stronger than that in the GNPs/ZnO samples.

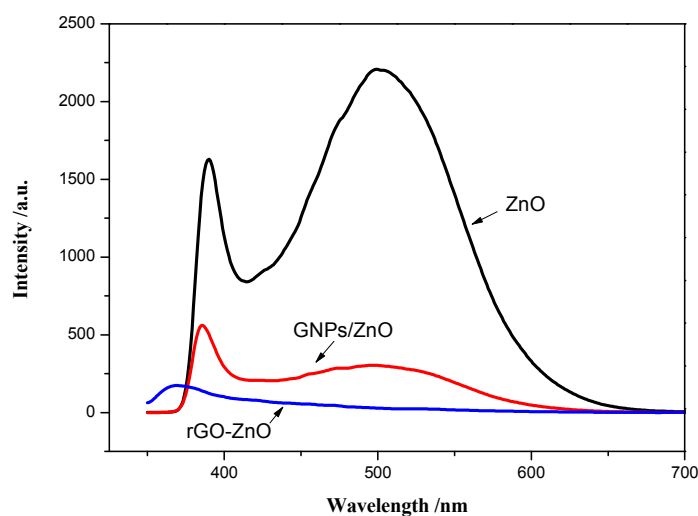


Figure 3 Photoluminescence (PL) spectra of ZnO, GNPs/ZnO and rGO-ZnO

The interaction between ZnO particles and rGO sheets were further investigated by the cyclic voltammetry (CV) test. It was reported in the literature that the intimate interaction between graphene and metal oxides could improve the specific capacitance of whole electrode [26-28]. In our rGO-ZnO samples, ZnO particles either coated on rGO surface or embedded between rGO layers can enhance the interaction with rGO. The CV curves of the rGO-ZnO electrode exhibited a quasi-rectangular shape, indicating good charge propagation at the electrode surface without obvious redox peaks [29], as shown in Figure 4(a). However, the curve of GNPs/ZnO electrode

showed a great eccentricity of the ellipse, even close to a straight line, indicating no significant capacitance characteristics. Obviously, the current response of rGO-ZnO samples was much higher than that of the GNPs/ZnO samples. The average current of rGO-ZnO samples was higher than that of the GNPs/ZnO samples at various different potentials, indicating that the strong chemical interaction between ZnO particles and rGO sheets. The maximal integral area of CV loop of rGO-ZnO electrode indicates that the samples produced positive synergistic effects in specific capacitance between ZnO and rGO.

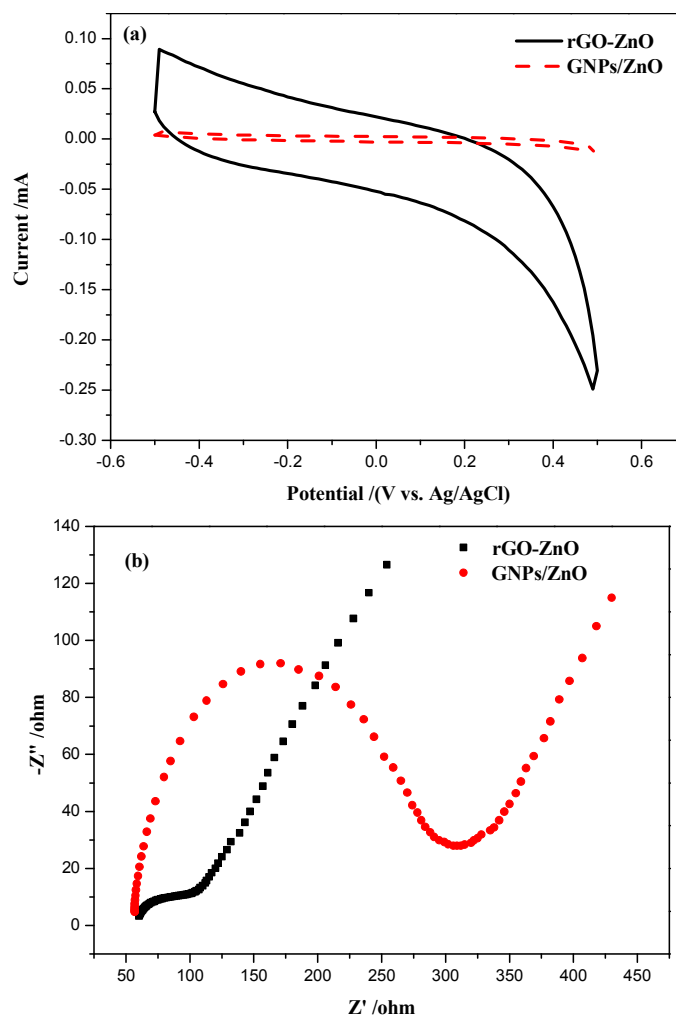


Figure 4 Cyclic voltammetric response (a) and Nyquist plots (b) of rGO-ZnO and GNPs/ZnO

To further exam the electron and ion transport in electrode materials, electrochemical impedance spectra (EIS) were also performed. The high-frequency corresponding to the charge transfer limiting process is ascribed to the pseudo-capacitance at the contact interface between electrode and electrolyte solution, while the straight line in the low frequency range is related to the diffusive resistance (Warburg resistance) of the electrolyte into the interior of the electrode and ion diffusion/transport into the electrode surface [30]. From the Nyquist plots shown in Figure 4b, the rGO-ZnO samples exhibited one depressed semicircle at high frequencies compared to the GNPs/ZnO samples. This indicates that the solid state interface layer resistance and charge-transfer resistance in the rGO-ZnO samples are lower than that in the GNPs/ZnO samples, which further confirms the strong interaction between ZnO particles and rGO.

3.2 Interfacial interaction of the PVC/rGO-ZnO composites

Figure 5 shows SEM images of the cryo-fracture surface of the PVC/rGO-ZnO samples and the PVC/GNPs/ZnO samples. As can be observed, the rGO-ZnO particles were well embedded in the polymer matrix without agglomeration, suggesting good compatibility and strong interfacial interaction between rGO-ZnO and the PVC matrix (Figure 5a and c). In contrast, the GNPs/ZnO particles agglomerated in the PVC matrix, indicating weak compatibility and interaction between the GNPs/ZnO and PVC matrix (Figure 5e and g). Because of the high interfacial interaction between rGO-ZnO particles and the PVC matrix, it is difficult to observe the particles in the PVC matrix only by the morphological observation. The corresponding EDS maps of Zn element were also given with the morphological images together. The results showed that the

uniform distribution of Zn was found in the PVC/rGO-ZnO samples (Figure 5b and d), while the significant agglomeration of Zn was observed in the PVC/GNPs/ZnO samples (Figure 5f and h). The results further proved that the well dispersion of rGO-ZnO particles in the PVC matrix and strong interfacial interaction between two components.

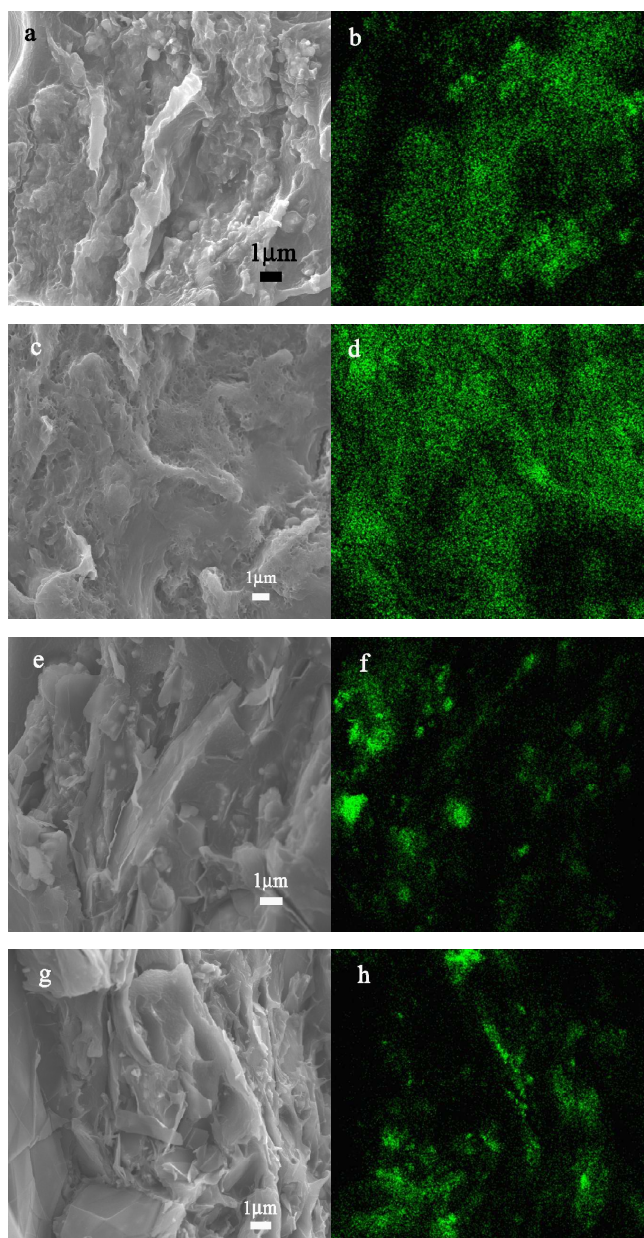


Figure 5 SEM images of the cryo-fracture surface of the PVC with 10 wt% (a) and 20 wt% (c) rGO-ZnO particles, the PVC with 10 wt% (e) and 20 wt% (g) GNPs/ZnO particles. (b), (d), (f) and (h) are corresponding Zn distribution of (a), (c), (e) and (g), respectively.

The interfacial interaction between rGO-ZnO particles and PVC was also evaluated by a thermodynamics study. The spreading coefficient (S_{a-b} , mN/m) of component a over component b was calculated by *equation 1* [31].

$$S_{a-b} = \gamma_b - \gamma_a - \gamma_{ab} \quad (1)$$

where γ_a and γ_b are the surface tensions of components a and b , respectively, and γ_{ab} is the interfacial tension between the two components. If S_{a-b} is positive, the component a will spread over component b , otherwise it will not. The γ_a and γ_b were calculated by *equation 2*.

$$(1 + \cos\theta)\gamma_i = 2\left(\sqrt{\gamma_s^d \gamma_i^d} + \sqrt{\gamma_s^p \gamma_i^p}\right) \quad (2)$$

where θ is the contact angle of a solid surface, and γ^d and γ^p are the dispersive and polar components of the surface tension, respectively. The interfacial tensions were calculated from the surface tensions of the components, using both harmonic-mean (*equation 3*) and geometric-mean (*equation 4*) equations [32, 33]. Furthermore, the spreading coefficients of the components were evaluated from both the harmonic and geometric interfacial tensions, as shown in Table 1.

$$\gamma_{12} = \gamma_1 + \gamma_2 - 4\left(\frac{\gamma_1^d \gamma_2^d}{\gamma_1^d + \gamma_2^d} + \frac{\gamma_1^p \gamma_2^p}{\gamma_1^p + \gamma_2^p}\right) \quad (3)$$

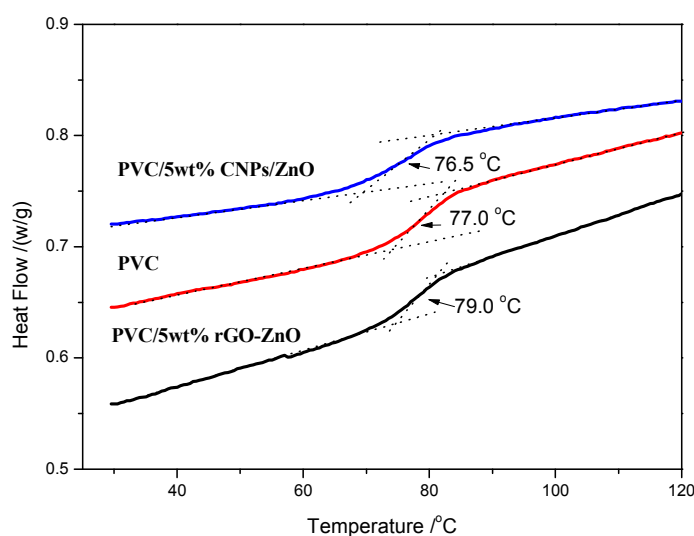
$$\gamma_{12} = \gamma_1 + \gamma_2 - 2\left(\sqrt{\gamma_1^d \gamma_2^d} + \sqrt{\gamma_1^p \gamma_2^p}\right) \quad (4)$$

The spreading coefficients of PVC with GNPs are negative, while the spreading coefficients of PVC with rGO-ZnO are positive. These results indicated that PVC could hardly spread over the GNPs surface but it could spread over the rGO-ZnO particles. Therefore, the above conclusions are consistent with the SEM observations.

Table 1 Surface tension, interfacial energy and spreading coefficient results of the composites

Samples	surface tensions /[mN/m]			interfacial energies with PVC /[mN/m]		spreading coefficient with PVC /[mN/m]	
	Total (γ)	dispersive part (γ^d)	polar part (γ^p)	harmonic	geometric	harmonic	geometric
PVC	43.2	42.0	1.2				
GNPs	51.8	38.6	13.2	10.14	6.51	-18.74	-15.11
rGO-ZnO	29.5	29.2	0.3	2.84	1.46	10.86	12.24

The enhancement of the interface interaction between PVC and rGO-ZnO particles is further investigated by analyzing their glass transition temperature (T_g). Figure 6 shows the T_g of PVC/GNPs/ZnO composites is close to the T_g of PVC, which is probably attributed to the weak interfacial interaction between the particles and PVC chains. In contrast, the T_g of PVC/rGO-ZnO increased from 77.0 to 79.0 °C at the same content of particles. The 2 K shifts in the glass transition temperature indicating that the chain segmental mobility of PVC was restrained by the strong interfacial interactions between the rGO-ZnO hybrid particles and PVC chains.

**Figure 6** The glass transition temperature of PVC, the PVC/5 wt% rGO-ZnO samples and the PVC/5 wt% GNPs/ZnO samples

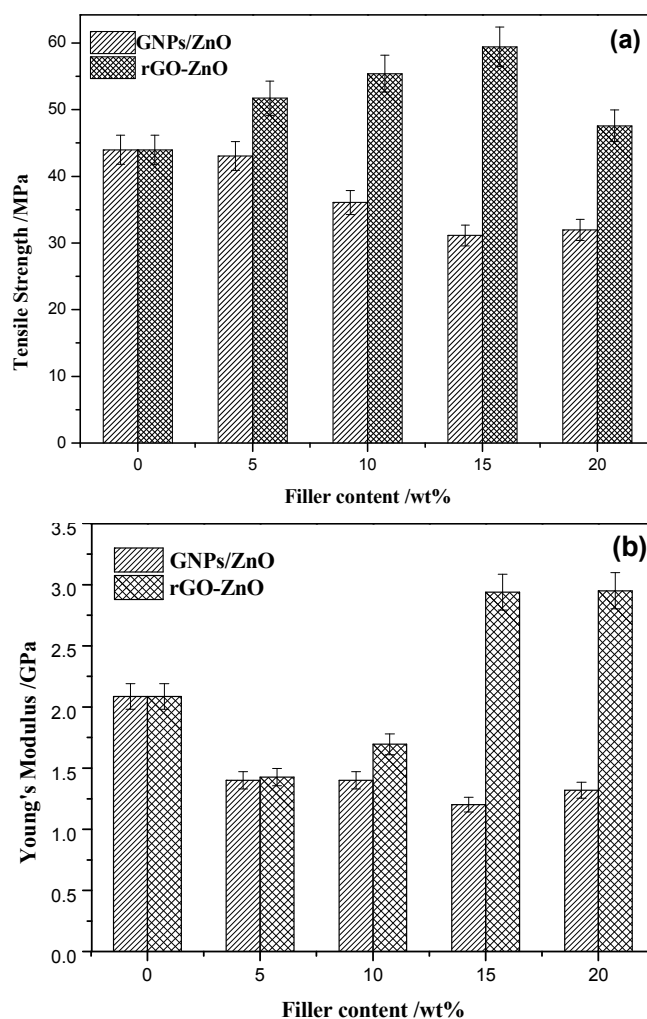


Figure 7 The tensile strength (a) and Young's Modulus (b) of PVC films containing the different fillers

The macro-scale properties of polymer composites are dependent on their nano- and micro-structures. The well dispersion and strong interfacial interaction between particles and polymer matrix usually lead to good mechanical properties of the polymer composites. Figure 7 shows the tensile strength and Young's modulus of the PVC films with rGO-ZnO fillers ranging from 5 to 20 wt% and the PVC films containing GNP/ZnO fillers. Clearly, the tensile strength of PVC with GNP/ZnO fillers decreased with the increase of the filler content because of the weak interaction and the aggregation of fillers. The tensile strength of PVC was reduced by 18 % after the

incorporation of 10 wt% GNPs/ZnO fillers. In contrast, the tensile strength of PVC was obviously improved by the incorporation of rGO-ZnO hybrids, even at high content of fillers (20 wt%). The tensile stress of PVC increased by 26 % and 8 % after the introduction of 10 wt% and 20 wt% rGO-ZnO hybrids particles, respectively. Furthermore, the incorporation of GNPs/ZnO particles showed negligible effect on the Young's modulus of PVC. However, the rGO-ZnO particles made the Young's modulus of PVC decrease only at low loading and the composites with high loading of rGO-ZnO particles possessed high Young's modulus. The incorporation of 15 wt% rGO-ZnO hybrid particles into the PVC could result in a 41.0 % increase of the Young's modulus.

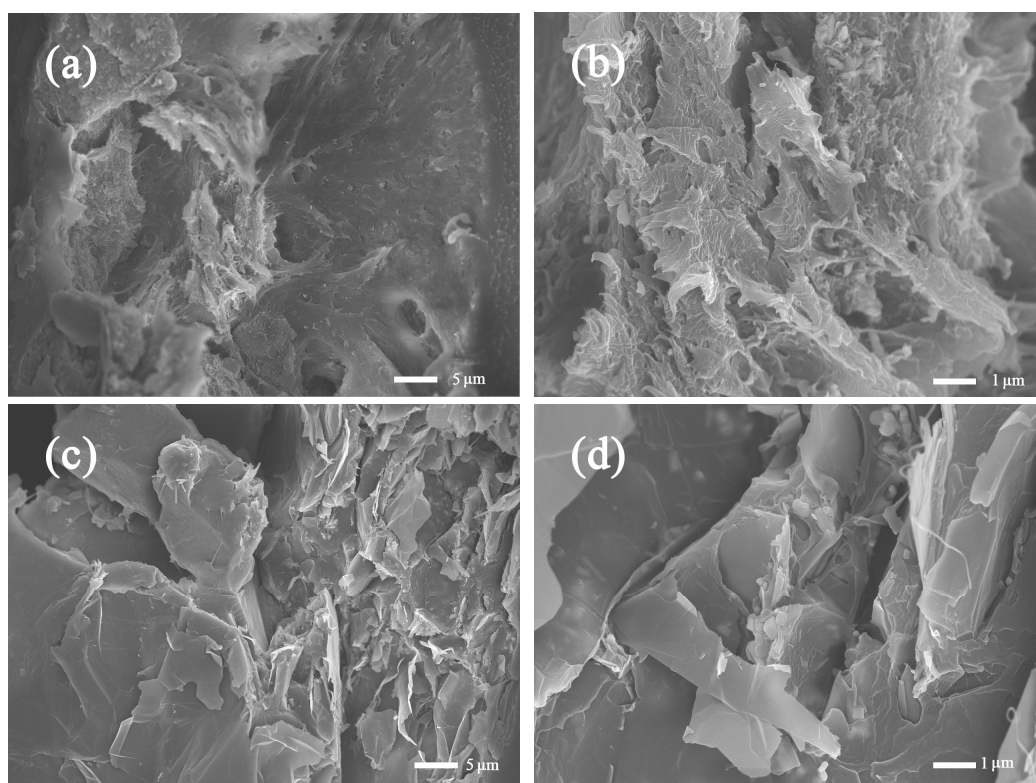


Figure 8 SEM images of the tensile fractured surface of the PVC with 10wt% rGO-ZnO particles (a, b) and the PVC with 10wt% GNPs/ZnO particles (c, d)

To explore the reasons for the mechanical enhancement by adding rGO-ZnO particles into PVC, the tensile fractured behavior of the PVC/rGO-ZnO composites and

the PVC/GNPs/ZnO composites were investigated, as shown in Figure 8. The fractured surfaces of the PVC/rGO-ZnO composites were very rough and the rGO-ZnO particles could be hardly distinguished from the PVC matrix (Figure 8a and b). However, for the PVC/GNPs/ZnO composites, the GNP surfaces were smooth and ZnO particles could be easily observed in the PVC/GNPs/ZnO composites (Figure 8c and d). These results indicated the strong interfacial interaction between rGO-ZnO particles and PVC chains but the weak interfacial interaction among GNPs, ZnO and PVC.

The above results indicate that the enhancement of tensile strength and Young's modulus in the PVC/rGO-ZnO composites was ascribed to the strong interfacial interaction. The presence ZnO particles play a key role in imparting strong interfacial interaction, which is fulfilled by strong p - π stacking interaction/electrostatic interaction with rGO and electrostatic interaction/hydrogen bonding with PVC. The Zn^{2+} ions first adsorbed onto the graphene surface by p - π stacking and electrostatic interactions. The formation of ZnO nanorods probably would not destroy these high interactions, resulting in the stable rGO-ZnO hybrid particles [34-36]. Furthermore, the ZnO had high dipole attraction and thus it can have favorable electrostatic interaction/hydrogen bonding with PVC chains [13, 14]. As a result, ZnO nanoparticles could play the role of a 'bridge' which connected rGO particles and PVC chains. For the PVC/GNPs/ZnO composites, the GNPs were quite smooth and the ZnO particles aggregated and showed weak interaction with PVC and GNPs, leading to weak connection between PVC chains and GNPs. Thus, the physical mixing of PVC, GNPs and ZnO can not exert the role of ZnO particles as a 'bridge' to connect PVC with GNPs.

4. Conclusions

In this work, we synthesized rGO-ZnO hybrid nanoparticles by a facile in situ hydrothermal route. A morphological study showed that, the single ZnO particles were well-established anchored on the rGO surface or embedded at interface of the rGO layers. As a result, the rGO-ZnO hybrid nanoparticles exhibited superior capacitive behavior and high interfacial interaction with PVC chains, compared with physical blending GNPs/ZnO particles. The tensile stress and Young's modulus of PVC had 35% and 41% increased by adding 15 wt% rGO-ZnO hybrid particles, respectively. The improvement of mechanical properties was mainly attributed to the enhancement of the interfacial interaction between rGO-ZnO hybrid nanoparticles and PVC chains via the 'bridge' effect of the ZnO particles, which had p - π stacking and electrostatic interaction with rGO particles and electrostatic attraction/hydrogen bonding with PVC chains. High interfacial interaction was also helpful to the nanoparticles evenly disperse in PVC matrix, and increased the glass transition temperature (T_g).

Acknowledgements

The authors are grateful to the National Natural Science Foundation of China (51103119), the Natural Science Foundation Project of CQ (CSTC2014JCYJA50024) and the Fundamental Research Funds for the Central Universities (XDJK2014B033) for financial support of this work.

References

- [1] Wilkes CE, Summers JW, Daniels CA, Berard MT. PVC handbook: Hanser Munich; 2005. p. 414-415.

- [2] Peprnicek T, Kalendová A, Pavlová E, Simonik J, Duchet J, Gerard JF. Poly (vinyl chloride)-paste/clay nanocomposites: Investigation of thermal and morphological characteristics. *Polymer Degradation and Stability* 2006;91(12):3322-3329.
- [3] Chazeau L, Cavaille J, Canova G, Dendievel R, Boutherein B. Viscoelastic properties of plasticized PVC reinforced with cellulose whiskers. *Journal of Applied Polymer Science* 1999;71(11):1797-1808.
- [4] Sun S, Li C, Zhang L, Du H, Burnell - Gray J. Interfacial structures and mechanical properties of PVC composites reinforced by CaCO₃ with different particle sizes and surface treatments. *Polymer International* 2006;55(2):158-164.
- [5] O'Connor I, Hayden H, O'Connor S, Coleman JN, Gun'ko YK. Kevlar coated carbon nanotubes for reinforcement of polyvinylchloride. *Journal of Materials Chemistry* 2008;18(46):5585-5588.
- [6] Zhu Y, Murali S, Cai W, Li X, Suk JW, Potts JR, Ruoff RS. Graphene and graphene oxide: synthesis, properties, and applications. *Advanced Materials* 2010;22(35):3906-3924.
- [7] Neto AC, Guinea F, Peres N, Novoselov KS, Geim AK. The electronic properties of graphene. *Reviews of Modern Physics* 2009;81(1):109.
- [8] Lau CN, Bao W, Velasco Jr J. Properties of suspended graphene membranes. *Materials Today* 2012;15(6):238-245.
- [9] Huang L, Li C, Yuan W, Shi G. Strong composite films with layered structures prepared by casting silk fibroin-graphene oxide hydrogels. *Nanoscale* 2013;5(9):3780-3786.

- [10] Sun J, Xiao L, Meng D, Geng J, Huang Y. Enhanced photoresponse of large-sized photoactive graphene composite films based on water-soluble conjugated polymers. *Chemical Communications* 2013;49(49):5538-5540.
- [11] Sternstein S, Zhu A-J. Reinforcement mechanism of nanofilled polymer melts as elucidated by nonlinear viscoelastic behavior. *Macromolecules* 2002;35(19):7262-7273.
- [12] Vaia RA, Maguire JF. Polymer nanocomposites with prescribed morphology: going beyond nanoparticle-filled polymers. *Chemistry of Materials* 2007;19(11): 2736-2751.
- [13] Olad A, Nosrati R. Preparation and corrosion resistance of nanostructured PVC/ZnO-polyaniline hybrid coating. *Progress in Organic Coatings* 2013;76:113-118.
- [14] Elashmawi I, Hakeem N, Marei L, Hanna F. Structure and performance of ZnO/PVC nanocomposites. *Physica B: Condensed Matter* 2010;405 (19):4163- 4169.
- [15] Zhang X-L, Zhao X, Liu Z-B, Shi S, Zhou W-Y, Tian J-G, Xu Y-F, Chen Y-S. Nonlinear optical and optical limiting properties of graphene oxide-Fe₃O₄ hybrid material. *Journal of Optics* 2011;13(7):075202.
- [16] Xie G, Xi P, Liu H, Chen F, Huang L, Shi Y, Hou F, Zeng Z, Shao C, Wang J. A facile chemical method to produce superparamagnetic graphene oxide-Fe₃O₄ hybrid composite and its application in the removal of dyes from aqueous solution. *Journal of Materials Chemistry* 2012;22(3):1033-1039.
- [17] Zhu J, Zeng G, Nie F, Xu X, Chen S, Han Q, Wang X. Decorating graphene oxide with CuO nanoparticles in a water-isopropanol system. *Nanoscale* 2010;2(6):988- 994.
- [18] Pendashteh A, Mousavi MF, Rahmanifar MS. Fabrication of anchored copper oxide

nanoparticles on graphene oxide nanosheets via an electrostatic coprecipitation and its application as supercapacitor. *Electrochimica Acta* 2013; 88: 347- 357.

[19] Hummers Jr WS, Offeman RE. Preparation of graphitic oxide. *Journal of the American Chemical Society* 1958;80(6):1339-1339.

[20] Wang Y-X, Chou S-L, Liu H-K, Dou S-X. Reduced graphene oxide with superior cycling stability and rate capability for sodium storage. *Carbon* 2013;57:202-208.

[21] Chen Y-L, Hu Z-A, Chang Y-Q, Wang H-W, Zhang Z-Y, Yang Y-Y, Wu H-Y. Zinc Oxide/Reduced Graphene Oxide Composites and Electrochemical Capacitance Enhanced by Homogeneous Incorporation of Reduced Graphene Oxide Sheets in Zinc Oxide Matrix. *The Journal of Physical Chemistry C* 2011;115(5):2563-2571.

[22] Eda G, Lin YY, Mattevi C, Yamaguchi H, Chen HA, Chen I, Chen CW, Chhowalla M. Blue photoluminescence from chemically derived graphene oxide. *Advanced Materials* 2010;22(4):505-509.

[23] Thomas HR, Day SP, Woodruff WE, Valles C, Young RJ, Kinloch IA, Morley GW, Hanna JV, Wilson NR, Rourke JP. Deoxygenation of Graphene Oxide: Reduction or Cleaning? *Chemistry of Materials* 2013;25(18):3580-3588.

[24] Prakash A, Bahadur D. The Role of Ionic Electrolytes on Capacitive Performance of ZnO-Reduced Graphene Oxide Nanohybrids with Thermally Tunable Morphologies. *ACS Applied Materials & Interfaces* 2014;6(3):1394-1405.

[25] Irimpan L, Nampoory V, Radhakrishnan P, Deepthy A, Krishnan B. Size dependent fluorescence spectroscopy of nanocolloids of ZnO. *Journal of Applied Physics* 2007;102(6):063524.

- [26] Yu G, Hu L, Liu N, Wang H, Vosgueritchian M, Yang Y, Cui Y, Bao Z. Enhancing the Supercapacitor Performance of Graphene/MnO₂ Nanostructured Electrodes by Conductive Wrapping. *Nano Letters* 2011;11(10):4438-4442.
- [27] Wang H, Cui L-F, Yang Y, Sanchez Casalongue H, Robinson JT, Liang Y, Cui Y, Dai H. Mn₃O₄-graphene hybrid as a high-capacity anode material for lithium ion batteries. *Journal of the American Chemical Society* 2010;132(40):13978-13980.
- [28] Zhu X, Zhu Y, Murali S, Stoller MD, Ruoff RS. Nanostructured reduced graphene oxide/Fe₂O₃ composite as a high-performance anode material for lithium ion batteries. *ACS Nano* 2011;5(4):3333-3338.
- [29] Ding J, Zhu S, Zhu T, Sun W, Li Q, Wei G, Su Z. Hydrothermal synthesis of zinc oxide-reduced graphene oxide nanocomposites for an electrochemical hydrazine sensor. *RSC Advances* 2015;5(29):22935-22942.
- [30] Li X, Wang Z, Qiu Y, Pan Q, Hu P. 3D graphene/ZnO nanorods composite networks as supercapacitor electrodes. *Journal of Alloys and Compounds* 2015; 620:31-37.
- [31] Harkins WD. *The physical chemistry of surface films*: Reinhold Publishing Corp., New York; 1952.
- [32] Fenouillot F, Cassagnau P, Majeste JC. Uneven Distribution of Nanoparticles in Immiscible Fluids: Morphology Development in Polymer Blends. *Polymer* 2009; 50:1333-1350.
- [33] Zhang S, Deng H, Zhang Q, Fu Q. Formation of Conductive Networks with Both Segregated and Double-Percolated Characteristic in Conductive Polymer Composites

with Balanced Properties. ACS Applied Materials & Interfaces. 2014; 6: 6835-6844.

[34] Huang Y, Chen Y, Hu C, Zhang B, Shen T, Chen XD, Zhang MQ. 'Bridge' effect of CdS nanoparticles in the interface of graphene-polyaniline composites. Journal of Materials Chemistry 2012;2:10999-11002.

[35] Zhou X, Shi T, Zhou H. Hydrothermal preparation of ZnO-reduced graphene oxide hybrid with high performance in photocatalytic degradation. Applied Surface Science. 2012;258(17):6204-6211.

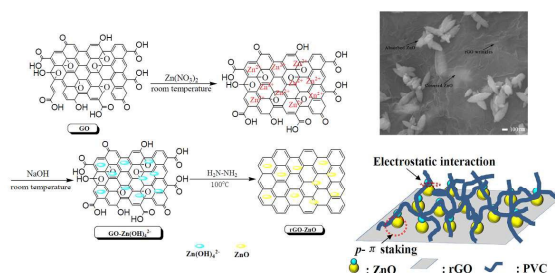
[36] Dey RS, Raj CR. A hybrid functional nanoscaffold based on reduced graphene oxide-ZnO for the development of an amperometric biosensing platform. RSC Advances 2013;3:25858.

Enhancement of Interfacial Interaction between Poly(vinyl chloride) and Zinc Oxide Modified Reduced Graphene Oxide

Ping Li¹ Xudong Chen^{1,2} Jian-Bing Zeng¹ Lin Gan¹ Ming Wang^{1*}

¹School of Chemistry and Chemical Engineering, Southwest University, Chongqing, 400715, China

² Key Laboratory of Polymer Composite and Function Materials of Ministry of Education, Key Laboratory for Designed Synthesis and Applied Polymer Materials, School of Chemistry and Chemical Engineering, Sun Yat-sen University, Guangzhou, 510275 China.



ZnO nanoparticles acted as a 'bridge', connecting with PVC chains and rGO sheets, to enhance the interfacial strength between them.

*Corresponding Author. Tel/Fax: 0086-023-68254000.
E-mail address: mwang@swu.edu.cn (M. Wang)